

ARTICLE

Received 24 Sep 2012 | Accepted 18 Mar 2013 | Published 30 Apr 2013

DOI: 10.1038/ncomms2758

OPEN

Calix[*n*]imidazolium as a new class of positively charged homo-calix compounds

Young Chun^{1,*}, N. Jiten Singh^{1,*†}, In-Chul Hwang^{1,†}, Jung Woo Lee¹, Seong Uk Yu¹ & Kwang S. Kim¹

Macrocycles based on neutral calixarenes and calixpyrroles have been extensively explored for ion binding, molecular assembly and related applications. Given that only these two types of calix compounds and their analogs are available, the introduction of new forms of widely usable calix macrocycles is an outstanding challenge. Here we report the quadruply/quintuply charged imidazole-based homo-calix compounds, calix[4/5]imidazolium. The noncovalent (C-H)⁺/π⁺-anion interactions of the imidazolium rings with anions inside and outside the cone are the stabilizing factors for crystal packing, resulting in self-assembled arrays of cone-shaped calix-imidazolium molecules. Calix[4]imidazolium senses fluoride selectively even in aqueous solutions. Calix[5]imidazolium recognizes neutral fullerenes through π⁺-π interactions and makes them soluble in water, which could be useful in fullerene chemistry. Not only derivatization and ring expansion of calix[*n*]imidazolium, but also their utilization in ionic liquids, carbene chemistry and nanographite/graphene exfoliation could be exploited.

¹Center for Superfunctional Materials, Department of Chemistry, Pohang University of Science and Technology, Pohang 790 784, Korea. * These authors contributed equally to this work. † Present addresses: Core Technology Laboratory, Samsung SDI Co., Ltd, Yongin 446-577, Korea (N.J.S.); Center for Nanomaterials, Sogang University, Seoul 121-742, Korea (I.-C.H.). Correspondence and requests for materials should be addressed to K.K. (email: kim@postech.ac.kr).

Two types of calix compounds, calixarenes and calixpyrroles, have been known for more than a century. Calixarenes have been widely used as ionophores and receptors^{1–3}. Their derivatives, including substituted benzene and benzene-like molecules such as calixpyridines, have been extensively explored for intriguing self-assembly of nanoelectronic and nanooptical materials, and various crystal structures exhibiting extraordinary architecture have been reported^{4–12}. Calixpyrroles have also been utilized as anion sensors¹³. A number of calixpyrrole-based supramolecules and their analogs including calixfurans, calixthiophenes, calixindoles and calixphyrins have been synthesized and used in diverse applications^{14–18}. Derivatization, ring expansion and substitution with various functional moieties have been important factors in the advancement of the anion-sensing abilities of calix compounds. Calix molecules, by virtue of their inherent nature, have been extensively explored toward not only the advancement in molecular recognition and supramolecular assembly *vis-à-vis* crystal engineering, but also toward their application in biological^{19–21} and environmental areas²² including ionophores, extractions and transports^{23–26}.

The molecular recognition by the two types of neutral calix compounds is generally based on neutral or charged hydrogen bonds. Neutral hydrogen bonds for anions occur through N-H...anion interaction by amide, pyrrole, urea, ammonium and guanidinium groups. The negatively charged moiety of N or O can provide hydrogen bonds with cations. On the other hand, recently, the (C-H)⁺...anion ionic H-bond by the imidazolium group has been explored to synthesize positively charged receptors^{27–33}. Mostly, the reported imidazolium-based receptors have one to four imidazolium moieties in the form of tweezers, dipodal, tripodal and other open forms. Until now, imidazolium-based macrocycles have received less attention than the open-form counterparts, while some examples of imidazolium-based pseudo-calix (or hetero-calix) compounds and cyclophanes have been reported^{31,34–39}. Utilization of the ionic H-bonding by imidazolium moieties, which is much stronger than the H-bonding of the pyrrole and urea moieties³¹, would improve the binding affinity for the anion. In particular, the design of receptors with an array of positively charged imidazolium moieties in calix form would enhance the binding affinity toward the anions, and the selectivity for anions could be varied depending on the cavity size⁴⁰.

However, despite the progress made in the development of imidazolium-based anion receptors in the last decade, a

truly imidazolium-based homo-calix compound, analogous to calix[*n*]arene defined as having a [*1_n*]metacyclophane skeleton⁴¹ and calix[*n*]pyrrole, is not yet reported. Here, we report the simple one-pot synthesis of quadruply and quintuply positively charged calix[4]imidazolium and calix[5]imidazolium, which have an array of four and five imidazolium moieties connected by methylene bridge, respectively. We investigated the binding affinity for fluoride⁴⁰ in aqueous solution. We show that calix[5]imidazolium enables neutral C₆₀ fullerenes to be soluble in water, and is used to recognize the neutral fullerenes and nanographite/graphene flakes through novel π⁺–π interaction⁴². In the future, these calix[*n*]imidazolium compounds and their derivatives could be applied in carbene chemistry^{43–47} as well as in applications requiring novel ionic liquids^{48,49}.

Results

Synthesis and single-crystal X-ray analysis. A simple one-pot synthesis provided a new type of positively charged imidazolium-based homo-calix compounds that were observed as a single-crystal structure of calix[4]imidazolium (I) in the form of a chloride salt, I·4Cl·X·H₅O₂ (X=Cl/Br=0.5Cl·0.5Br) and calix[5]imidazolium (II) in the form of a bromide salt, II·5Br·[F·H₅O₂]. This is the first example of a positively charged imidazolium-based homo-calix compound. We adopted a template-directed synthesis with the chloride and bromide anions in the ring closure reaction to synthesize the calix[4/5]imidazolium receptors^{35,36}. The anion receptor, [calix[4]imidazolium]-[tetrabromide] (I·4Br), was synthesized through the reaction of 1-(1*H*-imidazol-1-ylmethyl)-1*H*-imidazole and tetrabutylammonium-chloride (TBA-Cl) in dibromomethane (CH₂Br₂), followed by anion exchange with ammonium hexa-fluoro phosphate (NH₄PF₆). Finally, we succeeded in synthesizing the receptor I·4Cl·X·H₅O₂ through anion exchange with excess HCl aqueous solution (Fig. 1). The procedure to synthesize I·4Cl·X·H₅O₂ was also applied to synthesize II·5Br with the addition of tetrabutylammonium-bromide (TBA-Br) in the place of TBA-Cl (Fig. 1). Crystals of the anion receptors (I and II) were obtained by slow air drying of a water solution. The crystal structures of the anion receptors (I and II) were characterized by single-crystal X-ray diffraction analysis (Supplementary Data 1–3) and ¹H-NMR.

We have isolated a single-crystal structure of I·4Cl as I·4Cl·X·H₅O₂ [=I⁴⁺·4Cl⁻·X⁻·(H₅O₂)⁺] (Fig. 2). A quadruply positively charged organic macrocyclic molecule

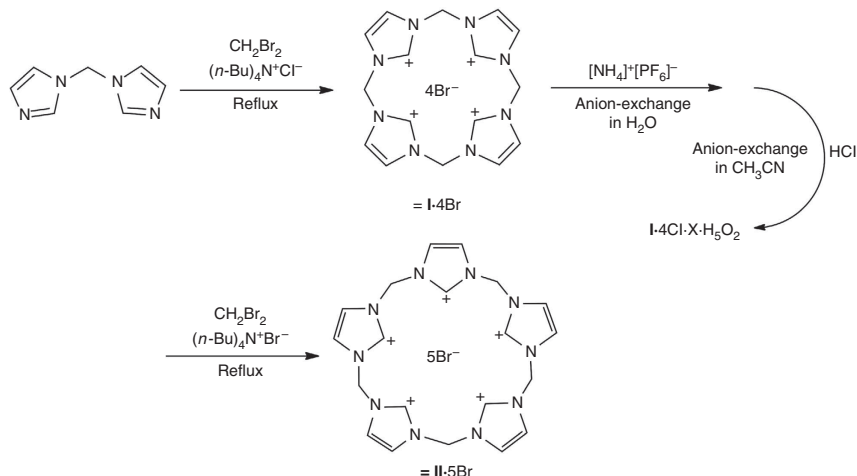


Figure 1 | Synthesis of I and II. An efficient one-pot synthesis generates a new type of positively charged imidazolium-based calix[*n*]imidazolium compounds.

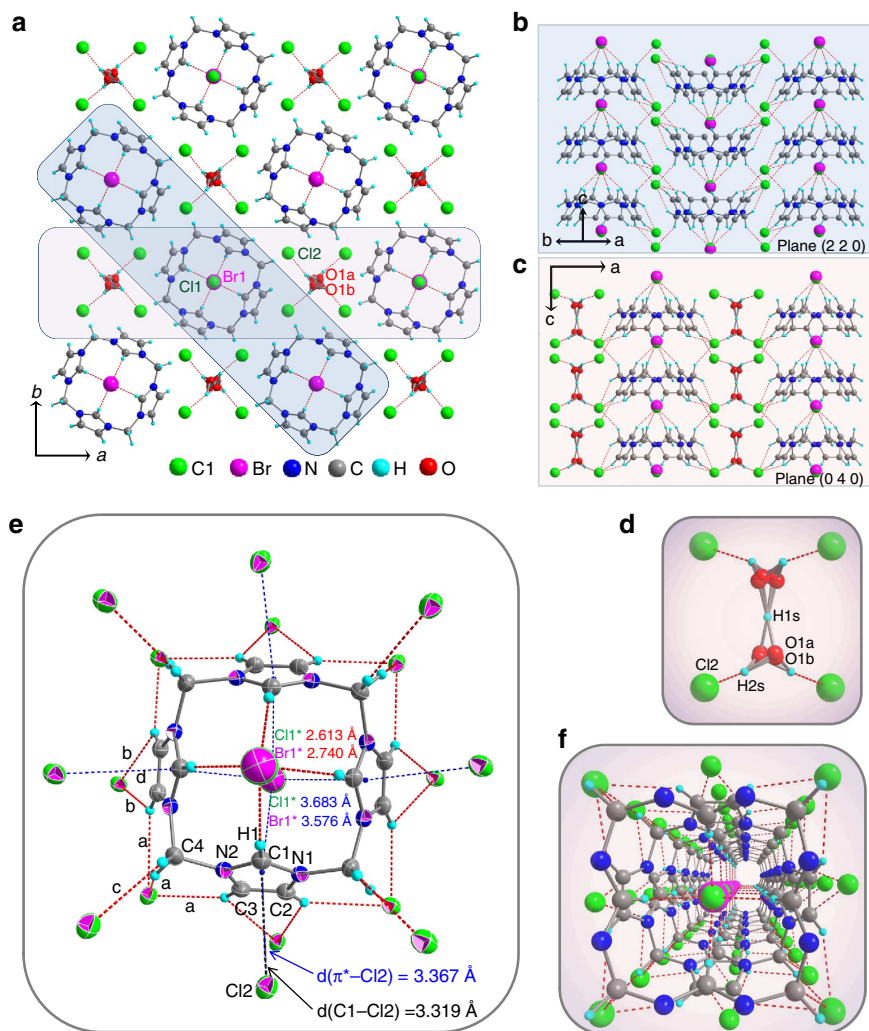


Figure 2 | X-ray crystal structures of $I \cdot 4Cl \cdot X \cdot H_5O_2$ ($X = Cl/Br$). (a) The unit cell structure of $(I^{4+} \cdot 4Cl^- \cdot X^-) \cdot (H_5O_2)^+$ viewed along the c -axis. Planes (220) and (040) are represented in shaded boxes. (b) Packing structure of $I \cdot 4Cl \cdot X \cdot H_5O_2$ on the plane (220). (c) Packing structure of $I \cdot 4Cl \cdot X \cdot H_5O_2$ on the plane (040). (d) Structure of $(H_5O_2)^+ \cdot 4Cl^-$. Dashed lines indicate H-bonds like ionic $Cl^- \cdots H_2O$. (e) Structure of $[I \cdot 4Cl \cdot X]^-$ showing different types of interactions. $a = 2.680, 2.731, 2.858 \text{ \AA}$, $b = 2.805, 3.136 \text{ \AA}$, $c = 2.686 \text{ \AA}$, $d = 3.367 \text{ \AA}$. (f) The perspective structure of arrays of $[I \cdot 4Cl \cdot X]^-$. In (b–f), the $(C-H)^+ \cdots X^-$ ionic H-bonds are in thick dashed red lines; $\pi^+ \cdots Cl^-$ interactions in thick dashed blue lines; $CH \cdots Cl^-$ H-bonds in thin dotted red lines. In (a), only the $(C-H)^+ \cdots X^-$ and $O-H \cdots Cl^-$ H-bonds are drawn in red color for visual clarity. As the Cl/Br is alternatively occupied, the corresponding O in H_5O_2 is positioned slightly differently, and so the O position is not given at a single point, but at four different points (O1a, O1b, O1a', O1b') in (d) close to each other; otherwise, a supercell needs to be used.

(I) in a tetragonal unit cell is surrounded by one $X(1)$, four $Cl(2)$ and one $(H_5O_2)^+$ (Fig. 2a). The cross sections of planes (220) and (040) in Fig. 2a denote the packing structures of the cone-shaped $I \cdot 4Cl \cdot X$ in Fig. 2b and c, respectively. When the structure is viewed through the b -axis, the cone conformations are arrayed in the same direction (Fig. 2c), while piled layers of cone conformations are arranged alternatively in opposite directions (Fig. 2b). In the packing pattern, each of the top $X(1)$ of $I \cdot 4Cl \cdot X$ has π^+ -anion interactions⁵⁰ with the quadruply positively charged π -system of the imidazolium moieties in $I \cdot 4Cl \cdot X$ (Fig. 2b). While each of the four $Cl(2)$ at the base of the cone conformation of $I \cdot 4Cl \cdot X$ has an extended coordination by forming a $CH \cdots Cl^-$ H-bond with a bridging CH_2 group of the second $I \cdot 4Cl \cdot X$ lying below. Four nearby units of $I \cdot 4Cl \cdot X$ surround a positively charged $(H_5O_2)^+$, which is charge-balanced by the neighboring Cl^- anions and stabilized by the $O-H \cdots Cl^-$ H-bonds. The $(H_5O_2)^+$ cation resides on a two-fold rotation axis of the Zündel-type structure (bond distances: $O1-H1s$ (1.172 \AA) and $O1 \cdots O1^a$ (2.34(1) \AA);

Fig. 2d). Altogether, the noncovalent interactions involving the $(C-H)^+ \cdots Cl^-$ ionic H-bond, the $C-H \cdots Cl^-$ H-bonds and the π^+ -anion interaction of X^- with four imidazolium rings are responsible for regular crystal packing toward the formation of an array of the cone-shaped $I \cdot 4Cl \cdot X$ units as a building block, where one chloride/bromide [$X(1)$] is bound at the top center of the cone and the chloride/bromide [$X(1)$] ion at the bottom center of the cone. The formation of the relatively small cavity size of the cone could be utilized for the recognition of small anions such as fluoride.

As seen in Fig. 2b, c and e, the receptor I forms a cone conformation of all four imidazolium $(C-H)^+$ moieties whose $(C-H)^+$ groups point toward the top $X(1)$ and whose rings face toward the bottom $X(1)$. Thus, $X(1)$ is octa-coordinated by four $(C-H)^+ \cdots X^-$ ionic H-bonds and four $\pi^+ \cdots X^-$ π^+ -anion interactions. The distance from a H-atom of the imidazolium $(C-H)^+$ group to the top $X(1)$ Cl^-/Br^- is 2.613/2.740 \AA , while the distances from the bottom X^- to the centroid of the positively charged imidazolium ring and the positively charged

C atom in the (C-H)⁺ group are 3.683/3.576 Å and 4.006/3.859 Å, respectively (Fig. 2e). Sixteen chloride atoms (Cl(2)) are located outside the cage of **I** with the aid of CH⁺⋯Cl⁻ H-bonds and the π⁺⋯Cl⁻ interaction, and these interaction distances are denoted as *a*–*d* in Fig. 2e, *a*: each of four Cl(2) anions is coordinated with the 3-H of an imidazolium moiety, the 4-H of the bridging CH₂ group and the 3-H of an adjacent imidazolium moiety at a distance of 2.680–2.858 Å, *b*: each of four Cl(2) anions is coordinated with the 2-H and 3-H of an imidazolium moiety at a slightly longer distance (2.805–3.136 Å), *c*: another four Cl⁻ anions are each coordinated with the second 4-H of the bridging CH₂ group in **I** at a distance of 2.686 Å, and *d*: each of four Cl⁻ anions forms a π⁺-anion interaction individually with the positively charged π-system of imidazolium moieties of **I** at the distance of 3.367 Å from the carbon atom of the (C-H)⁺ group. Each imidazolium moiety is hepta-coordinated with the top X(1) ((C-H)⁺⋯X⁻ ionic H-bond at the distance of 2.613/2.740 Å), the bottom X(1) (π⁺⋯X⁻ interaction at the distance of 3.683/3.576 Å), the Cl(2) (π⁺⋯Cl⁻ interaction at the distance of 3.367 Å) and the four CH⁺⋯Cl⁻ (2) interactions. Each of the Cl(2) anions has octa-coordination by six H-bonds surrounding the imidazolium moieties of **I**, one H-bond with (H₅O₂)⁺, and one π⁺⋯anion interaction. The cone conformations of **I**·4Cl⁻·X·H₅O₂ are stacked one above another continuously. This stacked structure results in a one-dimensional Cl⁻ array inside each pore comprising cavities (Fig. 2f) of stacked calix compounds.

The isolated crystal structure of the quintuply positively charged organic macrocyclic molecule (**II**) also adapted a cone conformation. It is composed of five different imidazoles connected through a methyl carbon. As in Fig. 3, the calix[5]imidazolium (**II**) has two types of interaction with the bromide anion that is located almost at the center of the cavity in this host molecule. The ionic H-bond interaction has three different distances from bromide to the hydrogen of imidazole (C-H)⁺, 3.242 Å toward H2, 3.684 Å toward H6 and 3.307 Å toward H10. The other interaction is π⁺⋯Br⁻ interaction between the imidazolium moiety and the bromide anion, which is an edge-to-face mode. Each of these three π⁺⋯Br⁻ interactions have distances of 3.711 Å, 3.541 Å and 3.708 Å,

respectively. These interactions stabilize the calix structure with a bromide anion centered in the cavity.

Water-soluble fullerene using calix[5]imidazolium (II). Given the strong π⁺–π interaction that has been explored in molecular recognition⁴², a bowl-shaped structure of calix[5]imidazolium led us to expect detection of fullerenes in aqueous solution. The spectroscopic results of fluorescence and NMR indicate that a boiling aqueous solution of **II**·5Br provides water-soluble fullerene (Supplementary Fig. S17–S19), which would be very useful for fullerene science. The fluorescence emission spectrum of C₆₀ in an aqueous solution of **II**·5Br showed an intensity enhancement, indicating the strong interaction between the calix[5]imidazolium (π⁺) and fullerene (π) systems. The chemical shift of the carbon in calix[5]imidazolium shows that the interaction takes place at the double bond of the imidazolium ring, not the (C-H)⁺ moiety of imidazolium. Every carbon in calix[5]imidazolium shifted downfield except for the carbon of imidazolium (C-H)⁺, while the characteristic single signal of fullerene in water was also observed. These results, which show an agreement with the calculated geometries (Supplementary Fig. S20), provide evidence for the interaction of the fullerene carbon cage and calix[5]imidazolium, as an important example of π⁺–π interaction contribution to the sensing process.

Recognition of aqueous fluoride by calix[4]imidazolium (I). To understand the binding features, we carried out isothermal titration calorimetry **I**·4Cl⁻·X·H₅O₂ toward the fluoride anion in aqueous solution at room temperature. The binding isotherm curve fitted the one-site model indicating a 1:1 complexation with a large binding constant of 8.3 × 10⁴ M⁻¹ (average value), as shown in Fig. 4 and Supplementary Fig. S1.

In a single-crystal structure, a unit cell includes an excess chloride and one (H₅O₂)⁺ ion. Thus, to investigate the influence of chloride, we prepared neutral **I**·4Cl by anion exchange with ammonium chloride (NH₄Cl). The calorimetric titration of this neutral **I**·4Cl still provided a large binding affinity of 2.5 × 10⁴ M⁻¹, though slightly smaller than the case of **I**·4Cl·X·H₅O₂, which implies that the excess chloride does not

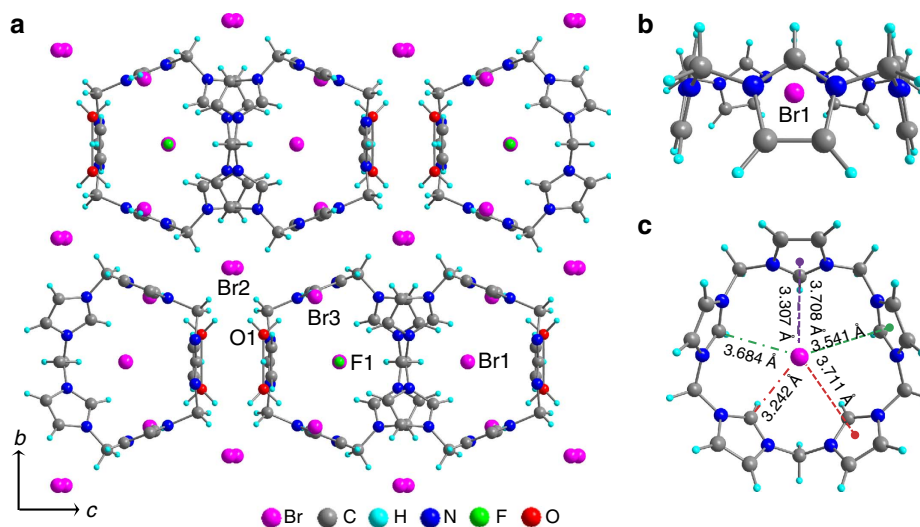


Figure 3 | X-ray crystal structures of **II·5Br·[F·H₅O₂].** (a) The unit cell structure viewed along the *a*-axis. A unit cell is denoted by a red box. (b) Side and top views of the structure of **II**·5Br·[F·H₅O₂] showing the (C-H)⁺⋯Br⁻ ionic H-bonds in thick dashed and dotted red line for Br1-H2, in green line for Br1-H6, and in violet line for Br1-H10, where the interactions are shown in thick dashed lines from the bromide anion to the centroid of an imidazole moiety.

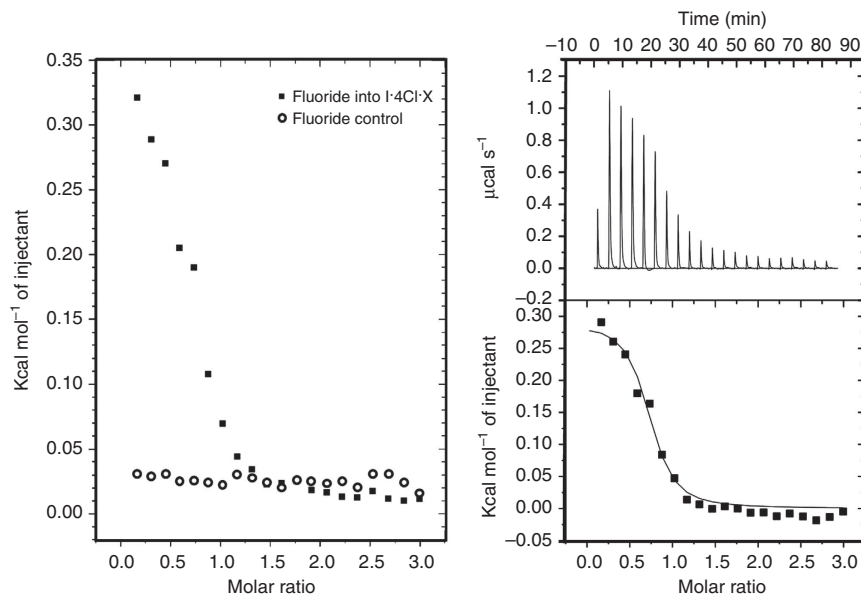


Figure 4 | Isothermal titration calorimetry (ITC) data of 0.5 mM $I \cdot 4Cl \cdot X \cdot H_5O_2$ ($= I \cdot 4Cl \cdot X$) in H_2O with 10 mM tetrabutylammonium fluoride (TBA-F). Left: ITC ΔH of 10 μ l injection of 10 mM TBA-F into 0.5 mM $I \cdot 4Cl \cdot X \cdot H_5O_2$ in water, experimental data (■) and control data (○). Right: ITC thermogram of TBA-F into $I \cdot 4Cl \cdot X \cdot H_5O_2$.

have a significant effect on the binding affinity toward F^- . Additionally, the calorimetric titration of neutral $I \cdot 4Cl$ with F^- in a slightly acidic buffered solution (where the neutral $I \cdot 4Cl$ was tuned to the 6.04 pH value with a 50 mM 2-(N-morpholino) ethanesulfonic acid (MES)/NaOH buffer solution, which has a similar pH to that of $I \cdot 4Cl \cdot X \cdot H_5O_2$) showed a titration curve very similar to the case of $I \cdot 4Cl \cdot X \cdot H_5O_2$. Finally, the calorimetric titrations of $I \cdot 4Br^-$ toward F^- provided a binding constant of $1.78 \times 10^4 M^{-1}$, which is still close to that of $I \cdot 4Cl \cdot X \cdot H_5O_2$ with F^- ($1.81 \times 10^4 M^{-1}$) in the presence of Br^- (in the form of TBA-Br). Therefore, the presence of excess chloride/bromide or other counter anions or protons does not have a significant effect on the binding of I with F^- (Supplementary Fig. S2–5 and Supplementary Table S1).

Furthermore, we checked the ^{19}F -NMR chemical shift changes of fluoride (TBA-F in D_2O) upon interacting with $I \cdot 4Cl \cdot X \cdot H_5O_2$, 1:1 molar ratio (Supplementary Fig. S6). The peak at -122.5 p.p.m. of the 10 mM TBA-F in D_2O slightly changed to -127 p.p.m. upon the addition of 1 molar equivalent of $I \cdot 4Cl \cdot X \cdot H_5O_2$. In addition, a new signal appeared at -147 p.p.m. due to the complexation of F^- with the receptor. Finally, the analysis of positive/negative electro-spray ionization mass spectrometry suggested the presence of 1:1 binding mode between $I \cdot 4Cl \cdot X \cdot H_5O_2$ and fluorides (Supplementary Fig. S8).

Variable-temperature NMR studies were performed to investigate possible conformers in solution for both **I** and **II** as Br^- and PF_6^- salts. Our variable-temperature NMR studies were done in the temperature ranges of 25 to 90 °C for Br^- salts in water (as Br^- salt is soluble only in water) and -40 to 75 °C for PF_6^- salts in acetonitrile:water (5:1) solvent mixture (Supplementary Fig. S25–28). In both cases, it seems that only one conformer is present in the solution over a wide range of temperatures; however, which form of the conformer would be present could not be rationalized from the NMR data.

We further attempted to correlate this data with the crystal data. We were able to isolate the crystal structure of an 1,2-alternate conformer of **I** in the presence of counterion (Br^-), unlike the observation of cone conformer obtained with excess

counterion (Cl^-) (due to HCl that was required for crystallization of the host). On the other hand, the 1,2-alternate conformer of $I \cdot 4Br$ is different from the cone conformer of **II** $\cdot 5Br$ salt observed in the crystal structure. For **I** or **II**, the existence of alternate and cone-conformers in solution or crystal depending on the counteranion seem to be controlled by the effectiveness in the ion-pair interaction between the host and $Cl^-/Br^-/PF_6^-$ anions (Supplementary Fig. S24: description).

Calix[4]imidazolium is able to make N-heterocyclic carbene (NHC) complexes. Silver complexes of NHC show antimicrobial activity⁴⁷ and are used as NHC transfer agents in transition metal chemistry⁴⁶. As a preliminary study, we identified the silver carbene complex of calix[4]imidazolium using 1H -NMR and ^{13}C -NMR (Supplementary Fig. S9).

Theoretical calculations. To understand the conformational structures of $I \cdot 4Cl$, $I \cdot 4Br$, $[I \cdot 5Cl]^-$ and $[I \cdot 4Cl \cdot F]^-$, we performed density functional theory (DFT) calculations (BLYP/6-31 + G^* level) for important conformational structures including two types of cone-conformers (c and t; c: one X^- is respectively coordinated from top and bottom of the cone, t: only one X^- is coordinated from the top of the cone), 1,2 and 1,3-alternate conformers (a12 and a13, respectively), and partial cone conformer (p) (Fig. 5, Supplementary Fig. S14 and Supplementary Table S7). The self-consistent reaction field-polarizable continuum model was used for the calculations in water. For $I \cdot 4Cl$, the most stable structure is $I \cdot 4Cl$ -c in the gas phase, but $I \cdot 4Cl$ -t in water (Fig. 5). In the cone conformer $I \cdot 4Cl$ -c, one Cl^- is bound at the top of the cone with $(C-H)^+ \cdots Cl^-$ ionic H-bonds and another Cl^- is bound at the bottom of the cone with the π^+ -anion interaction. In the $I \cdot 4Cl$ -t conformer, one Cl^- is bound at the top of the cone with $(C-H)^+ \cdots Cl^-$ ionic H-bonds and other three Cl^- anions are bound below with multiple $CH \cdots Cl^-$ H-bonds.

For $[I \cdot 5Cl]^-$, the cone conformer $[I \cdot 5Cl]^-$ -t, which is constructed by adding additional Cl^- in the $I \cdot 4Cl$ -t conformer, is the most stable conformer both in the gas phase and in water.

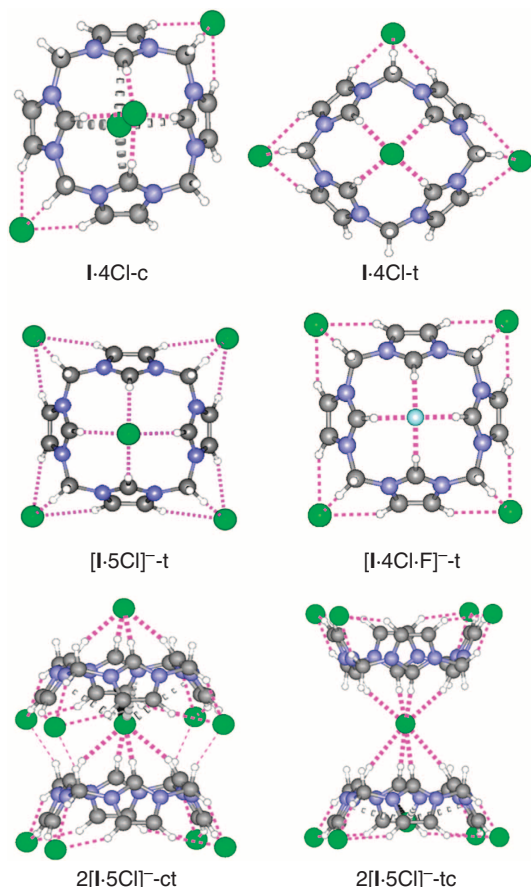


Figure 5 | B3LYP self consistent reaction field (SCRf) polarizable continuum model (PCM) optimized geometries of the cone-conformers of $\text{I}\cdot 4\text{Cl-c/t}$, $[\text{I}\cdot 5\text{Cl}]^{-\text{t}}$, $[\text{I}\cdot 4\text{Cl}\cdot \text{F}]^{-\text{t}}$, $2[\text{I}\cdot 5\text{Cl}]^{-\text{ct}}$ and $2[\text{I}\cdot 5\text{Cl}]^{-\text{tc}}$.

The $(\text{C-H})^+\cdots\text{Cl}^-$ ionic H-bonds and $\text{CH}\cdots\text{F}^-/\text{Cl}^-$ H-bonds are denoted by red dotted lines (distance ~ 2.7 Å or less); π^+ -anion interactions between Cl^- and positively charged imidazolium rings are in gray dotted lines. In aqueous solvent, $(\text{H}_5\text{O}_2)^+$ would not be present, so the water surrounding $[\text{I}\cdot 5\text{Cl}]^{-}$ was taken into account with SCRf PCM calculations.

For the binding mode of F^- with $\text{I}\cdot 4\text{Cl}$, the cone conformer $[\text{I}\cdot 4\text{Cl}\cdot \text{F}]^{-\text{t}}$ is much more stable than other conformers both in the gas phase and in water. Therefore, the 1:1 binding pattern of $[\text{I}\cdot 4\text{Cl}\cdot \text{F}]^{-}$ upon formation of complexes with $\text{I}\cdot 4\text{Cl}$ or $[\text{I}\cdot 5\text{Cl}]^{-}$ would be the cone form; for the latter case, one of the Cl^- would be replaced by the incoming F^- anion.

We also investigated the intriguing crystal packing in $\text{I}\cdot 4\text{Cl}\cdot \text{Cl}\cdot (\text{H}_5\text{O}_2)$ with DFT calculations (RI-B3LYP/TZVP level) for various structures of $[\text{I}\cdot 5\text{Cl}]^{-}$, $2[\text{I}\cdot 5\text{Cl}]^{-}$, $3[\text{I}\cdot 5\text{Cl}]^{-}$ and $4[\text{I}\cdot 5\text{Cl}]^{-}$ (Supplementary Fig. S15 and Supplementary Table S8). The Conductor-like Screening MOdel (COSMO) was used to treat the aqueous phase. As $[\text{I}\cdot 5\text{Cl}]^{-\text{t}}$ is the most stable conformer, it is conceivable that during crystal packing this conformer would have the most significant role apart from other important interaction involving the H_5O_2^+ moiety. As one $[\text{I}\cdot 5\text{Cl}]^{-\text{t}}$ approaches from below or top to another conformer, it would form the dimer $2[\text{I}\cdot 5\text{Cl}]^{-\text{ct}}$ (Supplementary Fig. S15) in which one of the Cl^- in between the two imidazolium rings is bound by four $(\text{C-H})^+\cdots\text{Cl}^-$ ionic H-bonds from below and by the π^+ -anion interaction with four positively charged imidazolium rings from above. Another form of the dimer, $2[\text{I}\cdot 5\text{Cl}]^{-\text{tc}}$, where one Cl^- has eight $(\text{C-H})^+\cdots\text{Cl}^-$ ionic H-bonds from two oppositely faced calix[4]imidazolium, is

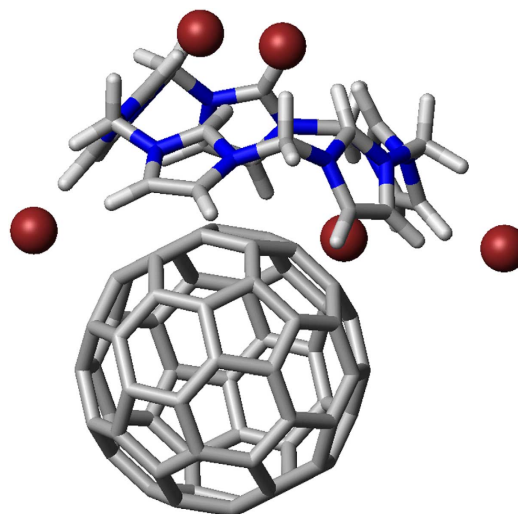


Figure 6 | The most stable geometry of the complex composed of the neutral C_{60} fullerene and $\text{II}\cdot 5\text{Br}$. Calculations were carried out with resolution identity-DFT.

unlikely to form as it is much less stable than the $2[\text{I}\cdot 5\text{Cl}]^{-\text{ct}}$ dimer (Fig. 5, Supplementary Fig. S15). Subsequent packing of $[\text{I}\cdot 5\text{Cl}]^{-\text{t}}$ either from above or below the $2[\text{I}\cdot 5\text{Cl}]^{-\text{ct}}$ dimer would lead to the formation of the trimer $(3[\text{I}\cdot 5\text{Cl}]^{-\text{ct}})$ (Supplementary Fig. S15). Further associations of a trimer or of two dimers would form the tetramer of $4[\text{I}\cdot 5\text{Cl}]^{-\text{ct}}$. Hence, step by step associations of monomers/n-mers of $[\text{I}\cdot 5\text{Cl}]^{-\text{t}}$ would elongate the packing to the infinite length, whereby each of the $[\text{I}\cdot 5\text{Cl}]^{-\text{t}}$ represents the building block of the crystal packing toward an infinite length of an array of cones.

We have also carried out the possible structures of $\text{II}\cdot 5\text{Br}$ interacting with the neutral C_{60} fullerene using resolution identity-DFT (Supplementary Fig. S20). The most stable structure is depicted in Fig. 6. The C_{60} fullerene matches well with the cavity size formed by five imidazole rings of II . The structure clearly shows the strong stacked $\pi^+-\pi$ interactions between the positively charged five imidazolium rings (π^+) and the aromatic fullerene carbon cage (π). When the $(\text{C-H})^+$ groups of imidazole rings interact with the fullerene cage, the structure is much less stable (Supplementary Fig. S20). This also explains why the fullerene is soluble in water by interaction with highly positively charged calix[5]imidazolium.

Discussion

We have synthesized the first quadruply positively charged homo-calix compound, calix[4]imidazolium in the form of a chloride salt ($\text{I}\cdot 4\text{Cl}\cdot \text{X}\cdot \text{H}_5\text{O}_2$). It has four positively charged imidazolium moieties to form a macrocycle connected through methyl bridges. The single X-ray crystal structure of $[\text{I}\cdot 4\text{Cl}\cdot \text{X}\cdot \text{H}_5\text{O}_2]$ elucidated that it had a cone-like conformation with all four imidazolium $(\text{C-H})^+$ groups pointing towards one chloride ion at the top of the center in the cavity, while their faces interacted with another chloride ion at the bottom in the cavity. The noncovalent interactions, that is, $(\text{C-H})^+\cdots\text{Cl}^-$ ionic H-bond, $\text{CH}\cdots\text{Cl}^-$ H-bonds, $\text{OH}\cdots\text{Cl}^-$ H-bonds and π^+ -anion interactions of Cl^- with four imidazolium rings of I from inside and outside of the cone, caused the crystal growth of negatively charged $(\text{I}\cdot 4\text{Cl}\cdot \text{X})^{-}$ and positively charged $(\text{H}_5\text{O}_2)^+$ of infinite length. This receptor displays excellent binding affinity for F^- in aqueous media revealing 1:1 binding stoichiometry between F^- and $\text{I}\cdot 4\text{Cl}\cdot \text{X}\cdot \text{H}_5\text{O}_2$, which was demonstrated by

isothermal titration calorimetry and DFT calculations. Molecular assembly phenomena utilizing calix[*n*]imidazolium as the building blocks by utilizing various forms of neutralizing counter anions should open a challenging task in crystal engineering.

We also synthesized an expanded ring compound, calix[5]imidazolium, which has a larger cavity size than calix[4]imidazolium, and characterized its X-ray structure. This expanded ring allows recognition of larger-size anions through electrostatic interactions. Importantly this calix[5]imidazolium enables neutral C₆₀ fullerenes soluble in water, and is used to recognize neutral fullerenes through novel $\pi^+ - \pi$ interactions, which have hardly been utilized in supramolecular chemistry. This interaction has been demonstrated by fluorescence and NMR spectroscopy as well as by theoretical calculations of the calix[5]imidazolium and fullerene complex. Eventually, this recognition could be utilized to diverse aromatic systems such as DNA bases, proteins and nanographite/graphene flakes (Supplementary Fig. S21). Therefore, these are indeed significant findings with possible wide applications in many branches of science.

Additionally, the synthesis of other forms of calix[*n*]imidazolium receptors by means of derivatization, incorporation with chromo/fluorogenic moieties, hydrophobic tails and expanded rings, (Supplementary Fig. S22) as well as its utilization in ionic liquids (Supplementary Fig. S23) and carbene chemistry should open a new field in supramolecular chemistry.

Methods

General procedures and synthesis. Imidazole, dibromomethane and tetrabutylammonium fluoride/chloride were purchased from Aldrich. ¹H-NMR and ¹³C-NMR spectra was performed on a Bruker Avance DPX500 (Bruker) (500 MHz) spectrometer at 298 K. ¹⁹F-NMR spectra were recorded on a Bruker Avance DPX300 (300 MHz) spectrometer at 298 K. VT ¹⁹F-NMR spectra were carried out on a Bruker Avance DPX500 (500 MHz) at 278, 298, 323, and 343 K. Electrospray ionization mass spectrometry spectra were recorded on a Agilent 6224 TOF LC/MS (Agilent). [Calix[4]imidazolium][pentachloride], I · 4Cl · X · H₂O₂ was synthesized as follows. Dibromomethane (10 ml, 9.79 mmol), 1-(1*H*-imidazol-1-ylmethyl)-1*H*-imidazole (3.5 mmol, 0.5 g) and tetrabutylammonium-chloride (7.2 mmol, 2 g) were mixed and the reaction mixture was stirred for 30 min. After stirring, the mixture was heated under reflux for 6 h. After cooling to room temperature, the precipitate was isolated and washed with fresh acetonitrile. The precipitate was dissolved in water (1 ml) and a saturated solution of ammonium hexa-fluoro phosphate (NH₄PF₆) (2 ml) was added to the solution. The resulting white precipitate was filtered off and washed with water. The product [calix[4]imidazolium][PF₆]₄ dissolved in acetonitrile was ion-exchanged with 12 N HCl solution. The obtained white-colored final product (I · 4Cl · X · H₂O₂) was recrystallized from water with a yield of 78.7%; ¹H-NMR (500 MHz, D₂O, 25 °C) δ 9.95 (s, 4H, imidazolium ring -N-CH-N-), δ 8.04 (s, 8H, imidazolium ring -N-CH-CH-N-), δ 6.92 (s, 8H, -N-CH₂-N-); ¹³C-NMR (500 MHz, D₂O) δ 59.81, 123.95, 139.56.

For the synthesis of [Calix[5]imidazolium][pentabromide] (II · 5Br⁻), 1-(1*H*-imidazol-1-ylmethyl)-1*H*-imidazole (3.5 mmol, 0.5 g) and tetrabutylammonium-bromide (7.7 mmol, 2.5 g) were added to dibromomethane (10 ml, 9.79 mmol), and the mixture was stirred for 30 min. After stirring, the mixture was heated under reflux for 6 h. After cooling to room temperature, the precipitate was isolated and washed with fresh acetonitrile. The final white-colored product was recrystallized from water with a yield of 75.3%; ¹H-NMR (500 MHz, D₂O, 25 °C) δ 9.99 (s, 5H, imidazolium ring-N-CH-N-), δ 8.07 (s, 10H, imidazolium ring-N-CH-CH-N-), δ 6.94 (s, 10H, -N-CH₂-N-); ¹³C-NMR (500 MHz, D₂O) δ 59.51, 123.64 and 139.47.

Fluorescence measurement. Fluorescence measurements were carried out at room temperature. The fluorescence emission spectra were performed with an aqueous solution of II · 5Br (24.8 mM, 10 ml) in the presence of fullerene (0.001 g, 1.38 μ mol), by monitoring the change in the intensity of fluorescence emission spectra. The fluorescence emission spectra were obtained using 389 nm excitation.

¹⁹F-NMR measurement. Fluorine NMR measurements were carried out at 298 K. The change in chemical shift of the solutions of 10 mM and 2 mM TBA-F in D₂O upon adding 1:1 molar equivalent of I · 4Cl · X · H₂O₂ in D₂O were recorded. The measurements were repeated at least twice to obtain consistent values. For the VT ¹⁹F-NMR, we prepared a 1:1 molar ratio of 250 mM I · 4Cl · X · H₂O₂ and 10 mM TBA-F, which were monitored at 278 K, 298 K, 323 K and 343 K, respectively.

Isothermal titration calorimetry. Every calorimetric titration was carried out using a fluoride control before titration of the calix[4]imidazolium receptor with respect to fluoride. The calorimetric titrations were repeated at least twice to obtain consistent values. For the calorimetric titrations of I · 4Cl · X · H₂O₂ and I · 4Br, we prepared 0.5 mM of each calix in water, and 10 mM TBA-F in water was added. For the titration of I · 4Cl, we prepared 1.0 mM I · 4Cl and 10 mM TBA-F in water as a starting concentration. For the case of I · 4Cl in the presence of buffer solution, we prepared 50 mM 2-(*N*-morpholino)ethanesulfonic acid (MES) buffer solution whose pH was 6.04 by manipulation with sodium hydroxide (NaOH). This MES buffer solution was used to make 0.5 mM of I · 4Cl and 10 mM TBA-F in a 50 mM MES buffer solution. For a competition study of halide anions, the calorimetric titration was carried out by adding 20 mM TBA-F into 1.0 mM I · 4Cl in the presence of 1.0 mM TBA-Br.

Theoretical calculations. The details of DFT calculation results are provided in the Supplementary Information.

References

- Lehn, J.-M. Supramolecular chemistry—scope and perspectives molecules, supermolecules, and molecular devices (Nobel Lecture). *Angew. Chem. Int. Ed.* **27**, 89–112 (1988).
- Shimizu, K. D. & Rebek, J. Synthesis and assembly of self-complementary calix[4]arenes. *Proc. Natl Acad. Sci. USA* **92**, 12403–12407 (1995).
- Schmidtchen, F. P. & Berger, M. Artificial organic host molecules for anions. *Chem. Rev.* **97**, 1609–1646 (1997).
- Vicens, J., Harrowfield, J. & Baklouti, L. *Calixarenes in the Nanoworld* (Springer, 2007).
- Prins, L. J., Huskens, J., de Jong, F., Timmerman, P. & Reinhoudt, D. N. Complete asymmetric induction of supramolecular chirality in a hydrogen-bonded assembly. *Nature* **398**, 498–502 (1999).
- Hong, B. H. *et al.* Self-assembled arrays of organic nanotubes with infinitely long one-dimensional H-bond chains. *J. Am. Chem. Soc.* **123**, 10748–10749 (2001).
- Hong, B. H., Bae, S. C., Lee, C. W., Jeong, S. & Kim, K. S. Ultrathin single-crystalline silver nanowire arrays formed in an ambient solution phase. *Science* **294**, 348–351 (2001).
- Sidorov, V. *et al.* Ion channel formation from a calix[4]arene amide that binds HCl. *J. Am. Chem. Soc.* **124**, 2267–2278 (2002).
- Casnati, A., Sansone, F. & Ungaro, R. Peptido- and glycolixarenes: playing with hydrogen bonds around hydrophobic cavities. *Acc. Chem. Res.* **36**, 246–254 (2003).
- Shivanyuk, A. Nanoencapsulation of calix[4]arene inclusion complexes. *J. Am. Chem. Soc.* **129**, 14196–14199 (2007).
- Lee, J. Y. *et al.* Near-field focusing and magnification through self-assembled nanoscale spherical lenses. *Nature* **460**, 498–501 (2009).
- Kral, V. *et al.* Calix[4]pyridine: a new arrival in the heterocalixarene family. *Chem. Commun.* 9–10 (1998).
- Gale, P. A., Sessler, J. L., Kral, V. & Lynch, V. Calix[4]pyrroles: old yet new anion-binding agents. *J. Am. Chem. Soc.* **118**, 5140–5141 (1996).
- Gale, P. A., Sessler, J. L. & Kral, V. Calixpyrroles. *Chem. Commun.* 1–8 (1998).
- Miyaji, H., Sato, W. & Sessler, J. L. Naked-eye detection of anions in dichloromethane: colorimetric anion sensors based on calix[4]pyrrole. *Angew. Chem. Int. Ed.* **39**, 1777–1780 (2000).
- Gale, P. A., Anzenbacher, P. & Sessler, J. L. Calixpyrroles II. *Coord. Chem. Rev.* **222**, 57–102 (2001).
- Sessler, J. L. *et al.* Crown-6-calix[4]arene-capped calix[4]pyrrole: an ion-pair receptor for solvent-separated Cs⁺ ions. *J. Am. Chem. Soc.* **130**, 13162–13166 (2008).
- Asfari, M.-Z. B. V., Harrowfield, J. & Vicens, J. *Calixarenes 2001* (Springer, Netherlands, 2001).
- Beer, P. D. & Schmitt, P. Molecular recognition of anions by synthetic receptors. *Curr. Opin. Chem. Biol.* **1**, 475–482 (1997).
- Wintergerst, M. P., Levitskaia, T. G., Moyer, B. A., Sessler, J. L. & Delmau, L. H. Calix[4]pyrrole: a new ion-pair receptor as demonstrated by liquid-liquid extraction. *J. Am. Chem. Soc.* **130**, 4129–4139 (2008).
- Sessler, J. L. *et al.* A calix[4]arene strapped calix[4]pyrrole: an ion-pair receptor displaying three different cesium cation recognition modes. *J. Am. Chem. Soc.* **132**, 5827–5836 (2010).
- Kishan, M. R., Rani, V. R., Kulkarni, S. J. & Raghavan, K. V. A new environmentally friendly method for the synthesis of calix(4)pyrroles over molecular sieve catalysts. *J. Mol. Catal. A-Chemical* **237**, 155–160 (2005).
- Wichmann, K. *et al.* Polyamine-based anion receptors: extraction and structural studies. *Coord. Chem. Rev.* **250**, 2987–3003 (2006).
- Seganish, J. L. *et al.* Regulating supramolecular function in membranes: calixarenes that enable or inhibit transmembrane Cl⁻ transport. *Angew. Chem. Int. Ed.* **45**, 3334–3338 (2006).
- Eller, L. R. *et al.* Octamethyl-octaundecylcyclo[8]pyrrole: a promising sulfate anion extractant. *J. Am. Chem. Soc.* **129**, 11020–11021 (2007).

26. Fowler, C. J. *et al.* Enhanced anion exchange for selective sulfate extraction: overcoming the Hofmeister bias. *J. Am. Chem. Soc.* **130**, 14386–14387 (2008).
27. Yoon, J., Kim, S. K., Singh, N. J. & Kim, K. S. Imidazolium receptors for the recognition of anions. *Chem. Soc. Rev.* **35**, 355–360 (2006).
28. Ihm, H. *et al.* Tripodal nitro-imidazolium receptor for anion binding driven by (C-H)(+)–X– hydrogen bonds. *Org. Lett.* **4**, 2897–2900 (2002).
29. Sato, K., Arai, S. & Yamagishi, T. A new tripodal anion receptor with C–H center dot center dot center dot X– hydrogen bonding. *Tetrahedron. Lett.* **40**, 5219–5222 (1999).
30. Kwon, J. Y. *et al.* Fluorescent GTP-sensing in aqueous solution of physiological pH. *J. Am. Chem. Soc.* **126**, 8892–8893 (2004).
31. Chellappan, K., Singh, N. J., Hwang, I. C., Lee, J. W. & Kim, K. S. A calix[4]imidazolium[2]pyridine as an anion receptor. *Angew. Chem. Int. Ed.* **44**, 2899–2903 (2005).
32. Vickers, M. S., Martindale, K. S. & Beer, P. D. Imidazolium functionalised acyclic ruthenium(II) bipyridyl receptors for anion recognition and luminescent sensing. *J. Mater. Chem.* **15**, 2784–2790 (2005).
33. Amendola, V. *et al.* A metal-based trisimidazolium cage that provides six C–H hydrogen-bond-donor fragments and includes anions. *Angew. Chem. Int. Ed.* **45**, 6920–6924 (2006).
34. Garrison, J. C., Simons, R. S., Kofron, W. G., Tessier, C. A. & Youngs, W. J. Synthesis and structural characterization of a silver complex of a mixed-donor N-heterocyclic carbene linked cyclophane. *Chem. Commun.* 1780–1781 (2001).
35. Alcalde, E., Ramos, S. & Pérez-García, L. Anion template-directed synthesis of dicationic [14]imidazoliophanes. *Org. Lett.* **1**, 1035–1038 (1999).
36. Ramos, S., Alcalde, E., Doddi, G., Mencarelli, P. & Perez-Garcia, L. Quantitative evaluation of the chloride template effect in the formation of dicationic [1(4)]imidazoliophanes. *J. Org. Chem.* **67**, 8463–8468 (2002).
37. Gong, H. Y., Rambo, B. M., Karnas, E., Lynch, V. M. & Sessler, J. L. A 'Texas-sized' molecular box that forms an anion-induced supramolecular necklace. *Nat. Chem.* **2**, 406–409 (2010).
38. Serpell, C. J., Cookson, J., Thompson, A. L. & Beer, P. D. A dual-functional tetrakis-imidazolium macrocycle for supramolecular assembly. *Chem. Sci.* **2**, 494–500 (2011).
39. Wong, W. W. H., Vickers, M. S., Cowley, A. R., Paul, R. L. & Beer, P. D. Tetrakis(imidazolium) macrocyclic receptors for anion binding. *Org. Biomol. Chem.* **3**, 4201–4208 (2005).
40. Cametti, M. & Rissanen, K. Recognition and sensing of fluoride anion. *Chem. Commun.* 2809–2829 (2009).
41. Brodesser, G. & Vögtle, F. Homocalixarenes and homocalixpyridines. *J. Inclusion Phenom. Macrocyclic Chem.* **19**, 111–135 (1994).
42. Kim, K. S., Singh, N. J., Min, S. K. & Kim, D. Y. Comprehensive energy analysis for various types of pi-interaction. *J. Chem. Theor. Comput.* **5**, 515–529 (2009).
43. Viciano, M. *et al.* An N-heterocyclic carbene/iridium hydride complex from the oxidative addition of a ferrocenyl-bisimidazolium salt: implications for synthesis. *Angew. Chem. Int. Ed.* **44**, 444–447 (2005).
44. Arnold, P. L. & Pearson, S. Abnormal N-heterocyclic carbenes. *Coord. Chem. Rev.* **251**, 596–609 (2007).
45. Youngs, W. J., Hindi, K. M., Panzner, M. J., Tessier, C. A. & Cannon, C. L. The medicinal applications of imidazolium carbene-metal complexes. *Chem. Rev.* **109**, 3859–3884 (2009).
46. Cazin, C. S. J., Citadelle, C. A., Le Nouy, E., Bisaro, F. & Slawin, A. M. Z. Simple and versatile synthesis of copper and silver N-heterocyclic carbene complexes in water or organic solvents. *Dalton Trans.* **39**, 4489–4491 (2010).
47. Hahn, F. E. & Jahnke, M. C. Heterocyclic carbenes: synthesis and coordination chemistry. *Angew. Chem. Int. Ed.* **47**, 3122–3172 (2008).
48. Pádua, A. A. H., Costa Gomes, M. F. & Canongia Lopes, J. N. A. Molecular solutes in ionic liquids: a structural perspective. *Acc. Chem. Res.* **40**, 1087–1096 (2007).
49. Baldelli, S. Surface structure at the ionic liquid-electrified metal interface. *Acc. Chem. Res.* **41**, 421–431 (2008).
50. Schneider, H. J., Schiestel, T. & Zimmermann, P. Host-guest supramolecular chemistry. 34. The incremental approach to noncovalent interactions: coulomb and van der Waals effects in organic ion pairs. *J. Am. Chem. Soc.* **114**, 7698–7703 (1992).

Acknowledgements

This work was supported by NRF (National Honor Scientist Program: 2010-0020414, WCU: R32-2008-000-10180-0) and KISTI (KSC-2011-G3-02). The useful help on X-ray refinement from Professor M. Kawano (Postech) is greatly acknowledged.

Author contributions

Y.C. synthesized and crystallized the compound, and performed and analyzed the calorimetric titration, NMR and fluorescence measurements. N.J.S. designed the molecule, analyzed the experimental data and performed theoretical calculations. I.C.H. analyzed the crystal structure. J.W.L. helped in the experiment. S.U.Y. designed the ionic liquid concept. K.S.K. designed the research and supervised the whole project.

Additional information

Accession codes: The Cambridge Crystallographic Data Center (<http://www.ccdc.cam.ac.uk/conts/retrieving.html>) hosts the crystallographic data for these compounds. The single-crystal diffraction data for **I** · 4Cl · X · H₅O₂, **II** · 5Br, and **I** · 4Br were deposited as CCDC-740391, CCDC-836759, and CCDC-916190 respectively.

Supplementary Information accompanies this paper on <http://www.nature.com/naturecommunications>

Competing financial interests: The authors declare no competing financial interests.

Reprints and permission information is available online at <http://npg.nature.com/reprintsandpermissions/>

How to cite this article: Chun, Y. *et al.* Calix[*n*]imidazolium as a new class of positively charged homo-calix compounds. *Nat. Commun.* **4**:1797 doi: 10.1038/ncomms2758 (2013).



This work is licensed under a Creative Commons Attribution-NonCommercial-ShareAlike 3.0 Unported License. To view a copy of this license, visit <http://creativecommons.org/licenses/by-nc-sa/3.0/>